

Short Strong Hydrogen Bonds in 2-Acetyl-1,8-dihydroxy-3,6-dimethylnaphthalene: An Outlier to Current Hydrogen Bonding Theory?

Jesper Sørensen,^{†,§} Henrik F. Clausen,^{‡,§} Rasmus D. Poulsen,^{‡,§} Jacob Overgaard,[§] and Birgit Schiøtt^{*,†,‡,§}

Center for Insoluble Protein Structures and Interdisciplinary Nanoscience Center, Department of Chemistry, University of Aarhus, 8000 Aarhus C, Denmark

Received: July 10, 2006; In Final Form: November 6, 2006

The environmental influence on the electronic character of two O–H···O hydrogen bonds in a β -diketone, 2-acetyl-1,8-dihydroxy-3,6-dimethylnaphthalene, is studied by low-temperature synchrotron X-ray diffraction and high-level density functional theory (DFT) calculations. It is revealed that one of the hydrogen bonds is very strong, yet partial localization is found. This result is analyzed by atoms in molecules (AIM) theory and applying the source function. Model compounds, with less steric strain, reveal that the strong hydrogen bond is not merely a result of steric compression.

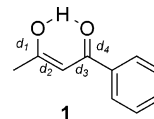
Introduction

The nature of the hydrogen bond (HB) has been a key issue in natural science for decades, since HBs are involved in numerous important contexts.¹ As an example the possible involvement of low-barrier hydrogen bonds (LBHBs) in enzyme catalysis has been much discussed.^{2–8} It has been proposed that the necessary requirements for LBHB formation is pK_a matching and a nonpolar environment.^{2,4,5} In a continued effort toward a unified HB theory, Gilli et al.⁹ have categorized all HBs as belonging to one of five classes: positive or negative charge-assisted hydrogen bonds (\pm CAHB), resonance-assisted hydrogen bonds (RAHB), polarization-assisted hydrogen bonds (PAHB), and isolated hydrogen bonds (IHB). Their studies have devoted particular attention to RAHB systems, where the unusual strength of the HB in neutral systems, such as β -diketones, is believed to originate from electron delocalization effects.⁹

We have an ongoing interest in the fundamental electronic nature of strong HBs and our main approach has been to combine very low-temperature, high-resolution X-ray and neutron diffraction experiments with high-level density functional theory (DFT) studies.¹⁰ By using the quantum theory of atoms in molecules (QTAIM)¹¹ to analyze the electron density (ED) of the β -diketone benzoylacetone, **1**, we were able to identify the partial covalent bond character of LBHBs.^{10a,b} It is generally believed that in very strong HBs the potential energy surface (PES) along the reaction coordinate is a single well.¹ Crystal structure correlations have shown that in such cases the HB becomes symmetric with a proton equally shared between the two heteroatoms.^{1c} In RAHB systems this is accompanied by a fully symmetric keto–enol fragment with complete delocalization.^{1d,9} Madsen et al.¹² studied nitromalonamide (NMA), which contains a very short RAHB ($d_{O-O} = 2.39$ Å). Although the keto–enol fragment of NMA is perfectly symmetric, it was surprisingly observed that the HB itself was quite

unsymmetric. However, this could be rationalized through the presence of intermolecular HBs to one of the key oxygen atoms.

Over the past decade, many attempts have appeared to establish empirical correlations between various properties of HBs. Efforts to correlate heteroatom distances to the strength of the hydrogen bond as measured either by ¹H NMR, by bond distance from neutron scattering experiments, or by theoretical calculations have been made.^{1,9} Correlations based on topological measures of the ED and the X···H distance have led to derivation of interatomic interaction potentials for HBs.¹³ For RAHB systems a key structure correlation is between d_{O-O} and the antisymmetric vibration parameter $Q = (d_1 - d_4) + (d_3 - d_2)$,⁹ **1**. An attractive feature of this index is that it does not require neutron diffraction data for accurate calculation, since it is based on the non-hydrogen atom positions. A particularly challenging problem has been to distinguish between short, strong, single-well HBs (e.g., NMA) and LBHBs (e.g., benzoylacetone, **1**) where the potential energy surface is characterized by two minima separated by a low barrier. Recently, QTAIM theory has been used to resolve this by application of the Bader and Gatti¹⁴ source function. The source function divides the ED at a point in space, for example, a bond critical point (BCP), into atomic contributions. It was shown that the character of the HB is correlated with the sign of the contribution from the hydrogen atom, negative for a weak (normal) HB and positive for a strong HB.¹⁴ LBHBs are clearly distinguished from short strong \pm CAHBs by showing an almost zero contribution to the ED from the hydrogen atom.¹⁴



In this paper we present the 15(2) K synchrotron X-ray diffraction structure of the β -diketone 2-acetyl-1,8-dihydroxy-3,6-dimethylnaphthalene, Figure 1. Single crystals were prepared from standard methods for self-condensation of diacetylacetone.¹⁵ This almost planar molecule is neutral, and like benzoylacetone, it packs in layers with large intermolecular

* To whom correspondence should be addressed: phone +45 8942 3953; fax +45 8619 6199; e-mail birgit@chem.au.dk.

[†] Center for Insoluble Protein Structures.

[‡] Interdisciplinary Nanoscience Center.

[§] Department of Chemistry.

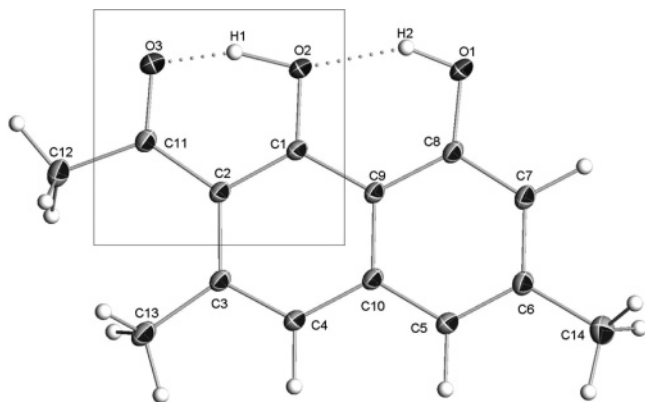


Figure 1. Structure of 2-acetyl-1,8-dihydroxy-3,6-dimethylnaphthalene at 15(2) K. Hydrogen atoms are placed on the basis of calculated positions from standard neutron data for O–H and C–H distances. Thermal ellipsoids for heteroatoms are drawn at the 90% level. The short hydrogen bond of interest is enclosed in the box. Atom numbering used throughout the study is shown.

distances; that is, it has very weak intermolecular interactions.¹⁶ Two short intramolecular O–H···O interactions are found in the molecule: one O···O distance is very short⁹ and must be termed a RAHB [2.4031(7) Å], while the other is short⁹ [2.6073(7) Å] and also a RAHB-type interaction. The very strong HB is among the shortest known O–H···O HBs, and as for NMA it falls outside the range typically associated with RAHBs.^{9c} Following the arguments above for NMA, one would thus expect the keto–enol fragment to be symmetric. Furthermore, since no intermolecular hydrogen bonds are present in the crystal, then the HB itself should also be expected to be symmetric.¹ As will be shown below, the keto–enol fragment is far from symmetric and the strong HB is a severe outlier relative to published RAHB correlations.⁹ One may argue that the presence of the aromatic rings of the naphthalene unit will affect the resonance assistance, thus not making it a true RAHB. But then one, of course, must also ask why the HB is then so short and presumably strong? For neutral systems, very strong HBs have been observed only if they are assisted by resonance.⁹ It was this fundamental discrepancy, a short O···O distance combined with apparent π -localization, that prompted us to carry out a detailed study of 2-acetyl-1,8-dihydroxy-3,6-dimethylnaphthalene. Further interest comes from the fact that the molecule possesses two O–H···O HBs of different electronic nature. This allows us to study in detail the difference in chemical environment between the two HBs. The core question bearing on all HB research is, what chemical environment forces the distinction between the two HB in this molecule? In other words, what are the essential structural characteristics that determine the shape of the PES of the HBs? We present an accurate very low-temperature synchrotron X-ray diffraction structure in combination with high-level DFT calculations. As no significant intermolecular contacts are observed in the crystal structure, gas-phase calculations represent a good model of a molecule in the crystal. To quantify differences between the HBs, the computed ED is analyzed by QTAIM and the source function. Finally, to evaluate the effects of the 3-methyl substituent on the structure of the remaining part of the molecule, model compounds lacking this group are analyzed.

Experimental Methods

Synthesis of 2-Acetyl-1,8-dihydroxy-3,6-dimethylnaphthalene. The synthesis was based on standard procedures for a self-condensation reaction of the diacetylacetone precursor.¹⁵ First

50 g of dehydroacetic acid was refluxed in 250 mL of 37% hydrochloric acid until the formation of carbon dioxide had stopped. After evaporation of the solvents, the remaining thick brown gel was dissolved in 100 mL of 10% sodium hydroxide solution. Barium hydroxide (120 g) was dissolved in boiling water and added to the solution. The formed yellow precipitate was dissolved in 15% hydrochloric acid and extracted by chloroform. The obtained yellow-orange phase was evaporated, giving a yellow-brown oil, which after distillation and recrystallization from ethanol gave 16 g of the diacetylacetone precursor.

Single crystals of 2-acetyl-1,8-dihydroxy-3,6-dimethylnaphthalene were obtained by heating the diacetylacetone (5 g) and a few drops of piperidine over a boiling water bath. Every half hour, 2 drops of piperidine was added. After 3 h the brown gel was dissolved in boiling glacial acetic acid, and upon cooling, yellow crystalline needles of 2-acetyl-1,8-dihydroxy-3,6-dimethylnaphthalene were produced. These were subsequently recrystallized in toluene to give larger crystals better suited for single-crystal X-ray diffraction experiments.

Synchrotron X-ray Diffraction. For the synchrotron X-ray data collection, a minute yellow single crystal ($0.05 \times 0.03 \times 0.03$ mm³) was mounted in protective oil on a glass fiber rod glued to a small copper wire. This assembly was mounted on a brass pin, which was placed on the goniometer of a Huber four-circle diffractometer at the ChemMatCARS beam line at the Advanced Photon Source (APS), Argonne National Laboratory, Argonne, IL. The crystal was cooled to 15(2) K in a cold He stream. The data collection was done in φ -scan mode with steps of 0.2° (1 s exposure) and fixed ω and χ angles. The detector distance was 7.36(1) cm. The diffracted intensity was recorded with a Bruker charge-coupled device (CCD) detector mounted on the 2 θ arm of the diffractometer. The maximum resolution was 1.13 Å⁻¹, and a total of 18 044 reflections were integrated with SAINT+.¹⁷ After integration, the data were corrected for oblique incidence into the CCD detector,¹⁸ and a ϕ -correction was performed with SADABS.¹⁷ Data were subsequently averaged and corrected for absorption with SORTAV.¹⁹ In the multipole modeling of the data, only reflections measured more than twice were included in the refinements.

Structure Refinement. The crystal structure was solved and preliminary refinements by use of the traditional spherical model were performed with the direct methods program suite SHELXL-TL.²⁰ For subsequent full-matrix least-squares multipolar refinement based on F^2 , the Hansen and Coppens multipole model, as implemented in the XD program,²¹ was used. The positional and displacement parameters for the non-hydrogen atoms of the initial structural model were refined with high-order data ($\sin \theta/\lambda > 0.8$ Å⁻¹) and kept fixed during the initial multipole refinements. The complexity of the refinement was gradually increased over a series of further refinements, and the final multipole model included refinement of all structural parameters and multipoles up to octupoles on all non-hydrogen atoms. Two radial parameters were introduced on the two types, sp² and sp³, of carbon atoms as well as on the oxygen atoms, leading to a total of 6 κ values. Hydrogen atom bond distances were constrained by use of tabulated neutron values,²² and each hydrogen atom was refined by use of one monopole and one bond-directed dipole. Hirschfeld's²³ rigid bond test shows that all ΔU values are less than 8×10^{-4} Å², where the largest values are found at the two methyl carbon atoms. A summary of the crystallographic details is given in Table 1, and the results have been deposited with the Cambridge Crystallographic Data Center (CCDC). Supplementary crystallographic data for this paper is

TABLE 1: Experimental Details of Crystallographic Measurements on 2-Acetyl-1,8-dihydroxy-3,6-dimethylnaphthalene

property	value
empirical formula	C ₁₄ H ₁₄ O ₃
temperature, λ	15(2) K, 0.42 Å
space group	P1
<i>a</i>	7.217(2) Å
<i>b</i>	7.502(2) Å
<i>c</i>	10.654(3) Å
α	88.745(4)
β	74.281(6)
γ	76.141(5)
<i>V</i> , <i>Z</i>	538.5(4) Å ³ , 2
linear absorption coefficient	0.0111 mm ⁻¹
<i>T</i> _{min} , <i>T</i> _{max}	0.993, 1.000
(sin θ/λ) _{max}	1.13 Å ⁻¹
no. of reflns collected	18 044
no. of independent reflns	6991 (<i>R</i> _{int} = 0.0297)
no. of reflns used [<i>I</i> > 2σ(<i>I</i>)]	5328
no. of parameters	460
<i>N</i> _{par} / <i>N</i> _{ref}	11.583
<i>R</i> _F , <i>R</i> _{wF} , <i>R</i> _{allF}	0.0314, 0.0331, 0.0406
<i>R</i> _{F2} , <i>R</i> _{wF2} , <i>R</i> _{allF2}	0.0463, 0.0661, 0.0483
goodness-of-fit	1.0467
max. residual	0.33 e/Å ³

contained in CCDC 294262 and can be obtained free of charge via www.ccdc.cam.ac.uk/datarequest/cif.

Theoretical Calculations

Calculations were carried out with the Gaussian 03²⁴ suite of programs at the B3LYP/6-31++G(d,p) level of theory,²⁵ with the experimental structure as the input structure. Tautomer **3** was generated by manually moving H1 to O3 and subsequently optimizing the geometry. The transition-state structure, **TS**, was located by using the QST2²⁶ method as implemented in Gaussian 03. All structures are fully optimized and the stationary points were assigned as minima or transition states from the number of imaginary frequencies: zero for all minima and exactly one for the TS. The zero-point vibrational energies were estimated by the harmonic oscillator approach in Gaussian 03. NMR chemical shifts values are computed by the GIAO²⁷ methodology and all shifts are reported relative to tetramethylsilane. For the atoms in molecules analysis, the program AIM2000²⁸ was used to locate and analyze critical points of the electron density distribution. The program PROAIMV, included in the AIMPACK²⁹ program suite, was used to calculate atomic charges as well as the contribution from each atomic basin to the charge density at the bond critical points under investigation.

Results and Discussion

X-ray Structure Analysis. High-quality 15(2) K synchrotron X-ray data for structural and multipole refinements were measured at the ChemMatCARS beamline at the Advanced Photon Source (APS) at the Argonne National Laboratory, Argonne, IL. The final structure is displayed in Figure 1. Elaborate crystallization efforts have been carried out to obtain a single-crystal suitable for neutron diffraction, but so far without success. Further discussion of the HB is therefore based on theoretical calculations, but comparison of the optimized structure with the coordinates of the non-hydrogen atoms obtained from the very accurate X-ray data provides a reliability check on the adequacy of the theoretical model. The X-ray data allows us to establish that no structural disorder is present in the crystal. For keto-enol systems it can be difficult, on the

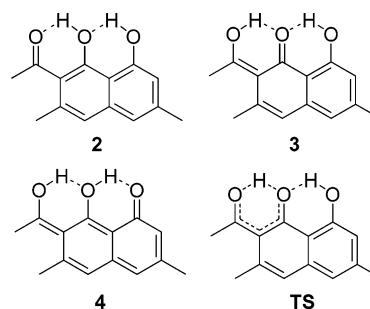
TABLE 2: Selected Interatomic Distances in Ångström (Å) for the Tautomers of 2-Acetyl-1,8-dihydroxy-3,6-dimethylnaphthalene^a

bond	2	3	TS	experiment
O3–H1	1.419	1.064	1.153	NA
O2–H1	1.040	1.366	1.229	NA
O3–O2	2.393	2.372	2.333	2.4031(7)
O2–H2	1.749	1.689	1.715	NA
O1–H2	0.977	0.988	0.984	NA
O2–O1	2.598	2.573	2.588	2.6073(7)
O3–C11	1.262	1.307	1.291	1.2635(6)
O2–C1	1.340	1.298	1.312	1.3374(6)
O1–C8	1.352	1.346	1.348	1.3594(6)
C11–C2	1.463	1.417	1.431	1.4666(7)
C2–C1	1.427	1.459	1.447	1.4254(8)
C1–C9	1.423	1.438	1.433	1.4339(7)
C9–C8	1.436	1.430	1.432	1.4365(8)

^a Complete list is found in Supporting Information.

basis of X-ray data, to distinguish between a symmetrically placed hydrogen atom and two partially occupied disordered hydrogens.³⁰ However, the latter case will also have disorder on the two oxygen sites due to the difference in bond lengths between single and double C–O bonds. In the crystal structure, refinement of such disorder will be absorbed in the atomic displacement parameters. Therefore, as pointed out by several authors, calculation of ΔU values along the bond direction provides a very sensitive probe for disorder.³¹ In the present case the ΔU values for C11–O3, C1–O2, and C8–O1 are 5×10^{-4} , 2×10^{-4} , and 3×10^{-4} Å², respectively, which clearly shows that these bonds are rigid. Gilli et al.^{9d} have suggested that the π -delocalization can be more easily traced by testing the rigidity of the carbon bonds in the enolone systems. Such a test gives values of 2×10^{-4} (C11–C2), 0×10^{-4} (C2–C1), and 1×10^{-4} Å² (C1–C9 and C9–C8), thus strongly indicating that no signs of static or dynamic disorder in the crystal is present.

Analysis of Tautomers. To fully account for the experimentally observed structure, we have studied all tautomers of 2-acetyl-1,8-dihydroxy-3,6-dimethyl-naphthalene, namely, **2**, the diphenolic tautomer, along with the two quinone-like tautomers, structures **3** and **4**. The analysis also included locating the transition state, **TS**, between **2** and **3**. Selected geometrical data of the optimized structures are found in Table 2 and in the Supporting Information.



All attempts to optimize tautomer **4** failed, as the hydrogen atom H2 consistently transferred back to the other oxygen atom, O1. Therefore data for this structure are not included in Table 2. This result shows that the HB between O1 and O2 must be classified as a normal electrostatic HB. The heteroatomic distances in tautomer **2** resemble very well the experimentally derived ones. This confirms that the level of theory applied is

TABLE 3: Computed Electronic Energies and ¹H NMR Chemical Shifts for the Different Tautomers

structure	2	3	TS	experiment
energy, ^a kcal/mol	0	0.87	1.01	NA
energy + ZPVE, ^b kcal/mol	2.55	2.52	0	NA
δ (H1), ^c ppm	18.8	20.4	22.7	17.5
δ (H2), ^c ppm	10.3	12.4	11.7	9.9

^a Energies are listed relative to **2**. ^b Electronic energies corrected for ZPVE are listed relative to **TS**. ^c ¹H NMR shifts (δ) are listed relative to TMS.³⁴

adequate for modeling the structure of the molecule. Previous calculations with a smaller basis set failed to give such a good correlation with the experimental structure, especially for the strong interaction.^{32a}

A structural evaluation of the two O–H···O interactions in **2** reveals that the left HB is indeed stronger as the O2–H1 bond is elongated considerably more than O1–H2, 1.040 Å compared to 0.977 Å. This fact is also represented in the heteroatom distances in the two bonds, being 2.393 Å and 2.598 Å, respectively, for the left strong HB and the right normal HB. The π -delocalization index, $\lambda = \frac{1}{2}(1 - Q/0.32)$,^{9a} for the –O–H···O= interaction is found to be 0.32 in **2** (O3···H1–O2) and 0.42 for both –O–H···O= systems present in **3**, O3–H1···O2 and O2···H2–O1.³³ Recalling, that a λ value of 0.5 indicates a fully delocalized ketoenolic system whereas λ values closer to 0 or 1 indicate localized bonding, it is seen that structure **3** has a more delocalized π -system than tautomer **2**. It is interesting to note that even though the two –O–H···O= systems in **3** have the same λ value, they differ by the fact that the shorter interaction, O3···H1–O2, shows almost identical carbon–oxygen distances, indicating the partial localization is due to differences in the two carbon–carbon distances, C1–C2 and C2–C11. For the O2···H2–O1 HB the situation is opposite, with the two carbon–oxygen distances, C8–O1 and C1–O2, being significantly different. By this, the molecule is able to conserve the aromatic character of the naphthalene unit.

Table 3 summarizes computed electronic energies, zero-point vibrational energies (ZPVE), and ¹H NMR chemical shifts for the tautomers. Structure **2** represents the tautomer with the lowest electronic energy, in agreement with the structural analysis above. The computed barrier for transfer of proton, H1, is very low between tautomers **2** and **3**, less than 1 kcal/mol in either direction. This indicates that H1 is probably shared between the two oxygen centers even at 15(2) K. Accurate single-crystal neutron diffraction data are required for unequivocal experimental verification. Calculation of zero-point vibration energies points in the same direction, as the O–H stretching frequencies are found to be well above the energy of the transition state, **TS**, giving rise to an effective single-well PES for O3···H1–O2. The computed numbers for this stretching frequency were 2484 cm⁻¹ (3.6 kcal/mol) and 2182 cm⁻¹ (3.1 kcal/mol) for **2** and **3**, respectively. Even though the approximation of a harmonic potential is not perfect, it is not expected that inclusion of anharmonicity in the calculation of the vibrational frequencies will change the overall picture, because the internal barrier is so low. On the basis of these DFT calculations, we suggest that the left HB in **2** is a double-well potential with a very low barrier between the two minima, so low that in practice the proton sits in a single-well potential. This is consistent with the experimental observation of a fully ordered crystal structure, without a fast dynamic transition between a carbon–oxygen single and double bond, as would

TABLE 4: Computed Molecular Properties at the Four Bond Critical Points Involved in Intramolecular Hydrogen Bonding for **2, **3**, and **TS****

molecular property ^a	bond critical point			
	O3–H1	H1–O2	O2–H2	H2–O1
ρ (2)	0.098	0.282	0.040	0.349
ρ (TS)	0.205	0.165	0.044	0.341
ρ (3)	0.264	0.112	0.048	0.337
∇ ² ρ (2)	0.142	-1.360	0.131	-2.079
∇ ² ρ (TS)	-0.637	-0.283	0.137	-2.013
∇ ² ρ (3)	-1.171	0.092	0.144	-1.972

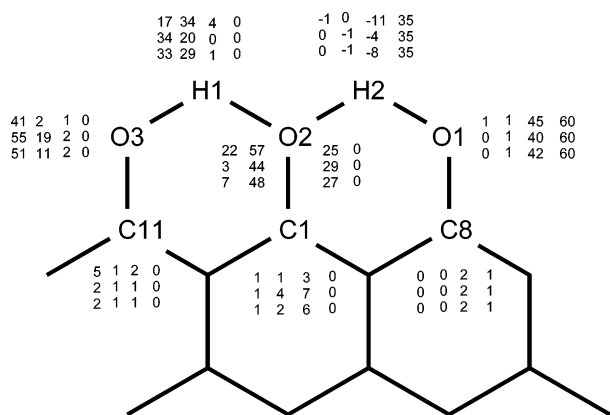
^a Electron density (ρ) and Laplacian (∇²ρ) values are reported in atomic units (au).

be the case if the hydrogen atom were found in a dynamical tautomeric equilibrium.

The computed ¹H NMR chemical shifts also point in the direction of a short strong HB as the numbers for tautomer **2** compare well with the experimentally determined solid-state chemical shifts. However, as pointed out by Pacios and Gómez,^{35a} a low-field proton NMR signal by itself cannot define the bonding character of a HB. Likewise, from computations on a saturated model system, Del Bene and co-workers^{35b} point out that such a chemical shift can be obtained without resonance assistance in the O–H···O hydrogen-bonded system. In the literature, attempts to correlate the NMR chemical shift directly to structural parameters are found. Mildvan et al.^{36a} have proposed an empirical formula for prediction of the heteroatom distance in O–H···O hydrogen-bonded systems. When applied to structure **2**, this formula fails for both of the intramolecular HBs in the system, systematically estimating the O···O distances too high by about 0.1–0.2 Å. Similarly, Gilli and co-workers^{36b} have published a relationship predicting the chemical shift from the O···O distance. For this system, the predicted chemical shifts are 18.4 and 11.4 ppm for δ(H1) and δ(H2), respectively, which are in good qualitative agreement with computed values for **2** and with the experimental shifts. We believe that the empirical formulas may be further improved by inclusion of the bonding angle of the hydrogen bond. When it deviates considerably from being linear, this will undoubtedly influence the deshielding of the proton and hence the measured NMR signal.

Atoms in Molecules Analysis. To gain further knowledge of the electronic nature of the two HBs in **2**, we turned our attention to QTAIM.¹¹ Selected density measures at the BCPs are compiled in Table 4. Only values related to the HBs are listed. It is evident that the H2···O2 interaction is a normal HB.^{13d,37} The very short HB, O3–H1···O2, on the other hand, has higher values for the ED at the BCP between H1 and both oxygen atoms, indicating a stronger interaction. The Laplacian shows the usual behavior^{10b} with two covalent bonds in the **TS** and only one in the two localized tautomers.

The last method used to characterize the two HBs is the source function.¹⁴ The computed values are listed in Chart 1 for the four BCPs associated with the two HBs. It is clear that O3–H1···O2 shows covalency in both of the O–H interactions, as positive contributions to the source function from H1 are calculated in both BCPs, between H1 and O3 and between H1 and O2. The trend is very clear and it is even revealed that, in the **TS**, the two bonds from H1 can be classified as “normal” O–H covalent bonds as judged by the sign and value of the source function, 33% and 29%. The other hydrogen-bonded system, O2–H2···O1, can be termed a normal electrostatic HB, as all tautomers show a negative contribution from H2 to the

CHART 1: Source Function Contribution to the Electron Density at Bond Critical Points of the Hydrogen Bonds^a

^a Percentage contributions from the eight labeled atoms are listed in matrices with rows corresponding to structures **2**, **3**, and **TS** and columns corresponding to the four hydrogen bonds. The first column describes the contribution to O3...H1, the second to H1...O2, the third to O2...H2, and the last to H2...O1. Only atoms contributing more than 1% are included.

O2–H2 electrostatic interaction and a large positive contribution to the covalent bond between H2 and O1.

It is important to note that when the contributions from the three hydrogen-bonded atoms are added in each of the four BCPs in Chart 1, they all add up to more than 80% of the total ED in all structures except for the electrostatic O2...H2 interaction. In this HB, only 59%, 65%, and 61% of the density in **2**, **3**, and **TS** originates from the three atoms in question. This is in line with the observation by Gatti and co-workers^{14b} that, for weaker hydrogen bonds, more atoms contribute to the density at the bond critical point. The remaining density originates from almost all other atoms in the molecule. Another interesting observation is the differences in the contributions from O2 to the O3–H1 and O1–H2 BCPs. In none of the three structures does O2 contribute to the normal O1–H2 interaction, whereas it has a significant contribution to the O3–H1 interaction in all three structures and most notably in **2**, in which it provides 22%. This indicates electron delocalization only in the left keto–enol fragment. Yet the asymmetry parameter, λ , points to comparable π -delocalization in both keto–enol systems in tautomer **3**. We speculate that these findings can be explained by the fact that only tautomer **2** allows for full delocalization in the naphthalene fragment. In order to keep the fully delocalized naphthalene system, C11–O3 has to be (mostly) of double-bond character and C1–O2 must be a single bond, which is found only in **2**. A consequence of this is that O3 is sp²-hybridized, thereby orienting a lone pair on O3 directly toward the H1–O2 hydrogen bond.

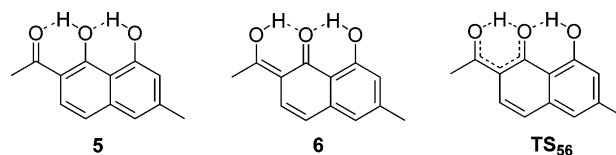
Model Compounds. One of the goals of this study is to reveal how the observed inconsistency between the experimental heteroatom separation, being short and indicative of a very strong interaction, and the accompanying π -delocalization parameters, pointing toward a localized system of a less strongly interacting system, can be explained structurally. A careful inspection of the structure of 2-acetyl-1,8-dihydroxy-3,6-dimethylnaphthalene, Figure 1, reveals that steric strain may be found in the compound between the 3-methyl group and the 2-acetyl group, as the two substituents in question are pushed apart. Ideally, the two angles C9–C3–C13 and C10–C2–C11 should be 180°; in the crystal structure these angles deviate by 4.96(4)° and 4.94(4)°, respectively. Therefore, calculations were

TABLE 5: Computed Structural Parameters for **5, **6**, and **TS₅₆****

parameter	5	6	TS₅₆
$d(\text{O3–H1})$, Å	1.524	1.042	1.163
$d(\text{O2–H1})$, Å	1.021	1.458	1.243
$d(\text{O3–O2})$, Å	2.469	2.434	2.358
$d(\text{O2–H2})$, Å	1.772	1.700	1.735
$d(\text{O1–H2})$, Å	0.978	0.988	0.983
$d(\text{O2–O1})$, Å	2.620	2.586	2.609
electronic energy, ^a kcal/mol	0.00	1.49	1.94
angle (C10–C2–C11), deg	178.5	178.7	177.4
λ^b	0.29	0.40	N/A
δ (H1), ppm	16.7	18.7	22.7
δ (H2), ppm	9.9	12.5	11.4
ρ (O3–H1), au	0.074	0.283	0.199
ρ (O2–H1), au	0.300	0.088	0.159
$\nabla^2\rho$ (O3–H1), au	0.166	–1.397	–0.619
$\nabla^2\rho$ (O2–H1), au	–1.590	0.055	–0.257

^a Energies are listed relative to **5**. ^b π -delocalization parameter.

set up for compounds where the 3-methyl group is not included: **5**, its tautomer **6**, and the transition state between the two, **TS₅₆**.

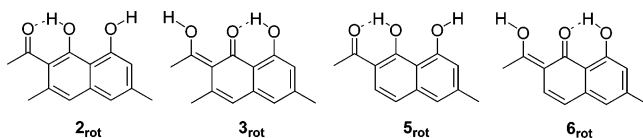


Computed structural parameters and electronic energies for the tautomers are shown in Table 5. As predicted above, the O2...O3 distance is indeed lengthened upon removal of C13 and the accompanying removal of the imposed steric strain between the substituents at the 2- and 3-positions in **2**. However, the heteroatom distance between O2 and O3, 2.469 Å, falls just inside the interval defined by Gilli and Gilli^{9c} for the short strong RAHB interactions. In line with this observation is the fact that the C10–C2–C11 angle is closer to being linear in the structures with no C13 methyl group; for comparison, angles of 174.8°, 174.5°, and 175.2° are computed in **2**, **3**, and **TS**.

The computed numbers reveal that the potential energy surface is a double well with a very low barrier of 1.9 kcal/mol between **5** and **6**. We do not believe that this slightly higher barrier is sufficient to change the overall appearance of the electronic characteristics of the molecule as other molecules, for example, benzoylacetone, has been shown to have a double well with an internal barrier of 2–3 kcal/mol and is characterized as an LBHB.^{10a,b,30} All structural and electron density parameters are essentially unchanged when the C13 methyl group is removed. The only major observed change is indeed the heteroatom distance of the short hydrogen bond and the NMR shift of H1 in the two tautomers. However, the distance still falls in the short range of a RAHB as defined by Gilli and Gilli,^{9c} and the value of the NMR shifts still reflect a strong hydrogen bond. Notably, the two transition states, **TS** and **TS₅₆**, show almost identical structural, topological, and spectroscopic features. Calculation of the source function for the structures further supports the presence of covalency between H1 and both oxygen atoms, O3 and O2. A positive contribution from H1 of 9% is computed for the H1...O3 interaction in **5**, and 15% is found for H1...O2 in **6**. The delocalization of the π -system is virtually unchanged upon removal of the C13 methyl group; numbers computed for λ are 0.02–0.03 lower for **5** and **6** when compared to those for **2** and **3**. The structural and topological analysis of the consequences of removal of C13 in 2-acetyl-

1,8-dihydroxy-3,6-dimethylnaphthalene thus points toward some relief of steric strain but without removing this apparent discrepancy between the trends in heteroatom distance and the π -delocalization parameter and maintaining a short HB.

Strength of Hydrogen Bond. The question now remains with respect to the strength of the hydrogen bond. It is not straightforward to compute the hydrogen bond energy of intramolecular hydrogen bonds, because any disruption of the bond will always be associated with a conformational change of the molecule and it is difficult to separate the energy differences into contributions from the formation of the hydrogen bond and the conformational change. Keeping this precaution in mind, we attempted to compute approximate hydrogen-bonding energies for 2-acetyl-1,8-dihydroxy-3,6-dimethylnaphthalene and the analogue where the 3-methyl group is removed. It is impossible to do simple rotations in tautomers **2** and **5** to break the short hydrogen bond; therefore approximate energies were extracted from conformations of **3** and **6** by generating conformers, **3_{rot}**, and **6_{rot}**, by simple rotation of the hydroxyl groups to break each of the short intramolecular hydrogen bonds. The results indicate indeed that the short hydrogen bond is strong — 22.1 kcal/mol in energy difference is computed between **3** and **3_{rot}** — whereas the longer hydrogen bond is weaker, as 9.5 kcal/mol is the calculated difference between **2** and **2_{rot}**. Relief of steric strain by removal of the 3-methyl group in **5** and **6** changes these two energy differences to 19.5 and 8.8 kcal/mol, respectively.



Recently a report on correlations between hydrogen bond energy and the topological parameters, electron density, or Laplacian at the hydrogen bond critical point were published.³⁸ Following the division in this report for the correlation between hydrogen bond energy and the electron density calculated in the bond critical point, the short hydrogen bond in 2-acetyl-1,8-dihydroxy-3,6-dimethylnaphthalene, tautomers **2** and **3**, must be termed a very strong hydrogen bond, whereas the one in the model compound, 2-acetyl-1,8-dihydroxy-6-methylnaphthalene, **5** and **6**, is bordering the ranges of a strong and a very strong hydrogen bond, both well above an estimated 20 kcal/mol.

The final method we have employed to evaluate the hydrogen bond energy of the two intramolecular hydrogen bonds is based on the empirical relationship $E_{\text{HB}} = -1/2V$,³⁹ in which V , the potential energy density in the bond critical point, can be extracted by use of the Abramov functional.⁴⁰ We have previously shown^{10e} that this method is comparable to extrapolating the energy from structural and topological correlations as well as computing from the theoretical wavefunction. Hydrogen bond energies of 41.4 kcal/mol for **2** and 27.9 kcal/mol for **5** are computed.

Conclusion

In conclusion, we have examined the two HBs in 2-acetyl-1,8-dihydroxy-3,6-dimethylnaphthalene by very low-temperature synchrotron X-ray diffraction and high-level DFT calculations. It is shown that the two intramolecular HBs are of different electronic nature. All the applied methods suggest that O1—H2 \cdots O2 must be termed a short normal (electrostatic) HB. Similarly, the O3—H1 \cdots O2 interaction appears to be a short strong covalent interaction, associated with a single-well PES

or a double-well PES with a proton-transfer barrier below the zero-point energies, resulting in an effective potential with only one (shared) position for the hydrogen atom. This finding is in accordance with the results from the Hirschfeld rigid-body test. A clear distinction between very short and strong covalent HBs and short electrostatic HBs is obtained by the source function, which gives (large) positive contributions from the hydrogen atom in question to both heteroatoms when they are covalently linked, similar to what has been found for benzoylacetone and nitromalonamide.^{10e} The present study indicates, however, that the keto—enol fragments lack full π -delocalization, which means that the conventional RAHB mechanism may not be strongly in play. It indicates that short strong hydrogen bonds can exist in neutral systems without taking advantage of a conjugated π -system, in line with the findings of Del Bene and co-workers.^{35b} RAHB may be a too-simplified way of looking at chemical bonding in such complex systems where aromatic fragments are parts of the β -diketone system. Such special systems should not just be left out of the overall picture for HB theory, as they may be able to tell us what other chemical components can be important in a molecule for formation of a short strong HB. The extreme strength of the O3—H1 \cdots O2 HB in this molecule may therefore (partially) have another electronic origin than RAHB,⁹ most likely associated with steric strain^{35b} or maybe the presence of the second phenol group. The presence of parts of an aromatic system within the β -keto—enol system also contributes to the formation of the strong interaction. We speculate that keeping a fully delocalized aromatic naphthalene π -system is more favorable than delocalizing the β -keto—enol fragment, as revealed by the differences in electronic energies between tautomers **2** and **3**, thereby forcing the two interacting oxygen atoms in close contact. Further studies of the topology of the Laplacian may provide deeper insights.

The consequence of removal of some of the imposed steric strain in 2-acetyl-1,8-dihydroxy-3,6-dimethylnaphthalene was examined in model compounds lacking the 3-methyl group. These results provided clear indications that the electronic character of the short HB cannot be attributed only to steric strain in the molecule. Along these lines, NMR measurements indicates that a similar molecule lacking both the 3-methyl group and the other hydroxyl group, 2-acetyl-1-hydroxynaphthalene, has a weaker HB, as a proton shift of 14.0 ppm has been reported.^{32b} It will be interesting to study the electronic effect of adding yet a third OH group to the structure. It can be speculated that a structure similar to **4** will then be stabilized, thereby strengthening the second HB. Studies along these lines are in progress in our group.

Acknowledgment. Allocations of beamtime at ChemMat-CARS at the Advanced Photon Source, Argonne National Laboratory, and computing resources through the DCSC installation at Aarhus University are acknowledged. Financial support from the Carlsberg Foundation, Danish National Research Foundation, and the Danish Natural Science Research Council is acknowledged. We thank Professor Dr. Jørgen Skibsted, University of Aarhus, for the NMR measurements, Marie-Agnes S. Chevallier for synthesis, as well as Dr. Yu-Sheng Chen and Dr. Tim Graber for assistance at APS. A referee is acknowledged for fruitful suggestions.

Supporting Information Available: Full list of all interatomic distances in the tautomers of 2-acetyl-1,8-dihydroxy-3,6-dimethylnaphthalene (S1) and 2-acetyl-1,8-dihydroxy-6-methylnaphthalene (S2), complete citation of Gaussian03, and all optimized structures. This material is available free of charge via the Internet at <http://pubs.acs.org>.

References and Notes

- (1) (a) Jeffrey, G. A. *An Introduction to Hydrogen Bonding*; Oxford University Press: Oxford, U.K., 1997. (b) Hibbert, F.; Emsley, J. *Adv. Phys. Org. Chem.* **1990**, *26*, 255–379. (c) Steiner, T. *Angew. Chem., Int. Ed.* **2002**, *41*, 48–76. (d) Sobczyk, L.; Grabowski, S. J.; Krygowski, T. M. *Chem. Rev.* **2005**, *105*, 3513–3560.
- (2) Cleland, W. W. *Biochemistry* **1992**, *31*, 317–319.
- (3) (a) Gerlt, J. A.; Gassman, P. G. *J. Am. Chem. Soc.* **1993**, *115*, 11552–11568. (b) Gerlt, J. A.; Gassman, P. G. *Biochemistry* **1993**, *32*, 11943–11952.
- (4) Cleland, W. W.; Kreevoy, M. M. *Science* **1994**, *264*, 1887–1890.
- (5) (a) Frey, P. A.; Whitt, S. A.; Tobin, J. B. *Science* **1994**, *264*, 1927–1930. (b) Frey, P. A. *Magn. Reson. Chem.* **2001**, *39*, S190–198.
- (6) Warshel, A.; Papazyan, A.; Kollman, P. A.; Cleland, W. W.; Kreevoy, M. M.; Frey, P. A. *Science* **1995**, *269*, 102–106.
- (7) Ash, E. L.; Sudmeier, J. L.; De Fabo, E. C.; Bachovchin, W. W. *Science* **1997**, *278*, 1128–1132.
- (8) (a) Kuhn, P.; Knapp, M.; Soltis, S. M.; Ganshaw, G.; Thoene, M.; Bott, R. *Biochemistry* **1998**, *37*, 13446–13452. (b) Bachovchin, W. W. *Magn. Reson. Chem.* **2001**, *39*, S199–S213. (c) Molina, P. A.; Jensen, J. H. *J. Phys. Chem B* **2003**, *107*, 6226–6233. (d) Yuan, C.; Tu, S.; Gelb, M. H.; Tsai, M.-D. *Biochemistry* **2005**, *44*, 4748–4754.
- (9) (a) Gilli, G.; Bellucci, F.; Ferretti, V.; Bertolasi, V. *J. Am. Chem. Soc.* **1989**, *111*, 1023–1028. (b) Gilli, P.; Bertolasi, V.; Ferretti, V.; Gilli, G. *J. Am. Chem. Soc.* **1994**, *116*, 909–915. (c) Gilli, G.; Gilli, P. *J. Mol. Struct.* **2000**, *552*, 1–15. (d) Gilli, P.; Bertolasi, V.; Pretto, L.; Ferretti, V.; Gilli, G. *J. Am. Chem. Soc.* **2004**, *126*, 3845–3855.
- (10) (a) Schiøtt, B.; Iversen, B. B.; Madsen, G. K. H.; Bruice, T. C. *J. Am. Chem. Soc.* **1998**, *120*, 12117–12124. (b) Schiøtt, B.; Iversen, B. B.; Madsen, G. K. H.; Larsen, F. K.; Bruice, T. C. *Proc. Natl. Acad. Sci. U.S.A.* **1998**, *95*, 12799–12802. (c) Overgaard, J.; Schiøtt, B.; Larsen, F. K.; Schultz, A. J.; MacDonald, J. C.; Iversen, B. B. *Angew. Chem., Int. Ed.* **1999**, *38*, 1239–1242. (d) Overgaard, J.; Schiøtt, B.; Larsen, F. K.; Schultz, A. J.; MacDonald, J. C.; Iversen, B. B. *Angew. Chem.* **1999**, *111*, 1321–1324. (e) Overgaard, J.; Schiøtt, B.; Larsen, F. K.; Iversen, B. B. *Chem.—Eur. J.* **2001**, *7*, 3756–3767. (f) Schiøtt, B. *Chem. Commun.* **2004**, 498–499. (g) Schiøtt, B.; Overgaard, J.; Larsen, F. K.; Iversen, B. B. *Int. J. Quantum Chem.* **2004**, *96*, 23–31.
- (11) Bader, R. F. W. *Atoms in Molecules. A Quantum Theory*; Oxford University Press: New York, 1990.
- (12) Madsen, G. K. H.; Wilson, C.; Nymand, T. M.; McIntyre, G. J.; Larsen, F. K. *J. Phys. Chem. A* **1999**, *103*, 8684–8690.
- (13) (a) Espinosa, E.; Molins, E. *J. Chem. Phys.* **2000**, *113*, 5686–5694. (b) Espinosa, E.; Alkorta, I.; Elguero, J.; Molins, E. *J. Chem. Phys.* **2002**, *117*, 5529–5542. (c) Mallinson, P. R.; Smith, G. T.; Wilson, C. C.; Grech, E.; Wozniak, K. *J. Am. Chem. Soc.* **2003**, *125*, 4259–4270. (d) Tang, T.-H.; Deretey, E.; Jensen, S. J. K.; Csizmadia, I. G. *Eur. Phys. J. D* **2006**, *37*, 217–222.
- (14) (a) Bader, R. F. W.; Gatti, C. *Chem. Phys. Lett.* **1998**, *287*, 233–238. (b) Cargnoni, F.; Gatti, C.; Bertini, L. *J. Comput. Chem.* **2003**, *24*, 422–436. (c) Gatti, C. *Z. Kristallogr.* **2005**, *220*, 399–457. (d) Gatti, C.; Bertini, L. *Acta Crystallogr.* **2004**, *A60*, 438–449.
- (15) Bethell, J. R.; Maitland, P. *J. Chem. Soc.* **1962**, 3751–3758.
- (16) Müller, G.; Lutz, M.; Lachman, J. *Acta Crystallogr.* **1994**, *C50*, 1318–1320.
- (17) Sheldrick, G. M. *SAINT* v6.36A, *SADABS* v2.05 and *SHELXTL* v6.10 programs included in the Bruker SMART CCD software, 2003.
- (18) Wu, G.; Rodrigues, B. L.; Coppens, P. *J. Appl. Crystallogr.* **2002**, *35*, 356–359.
- (19) Blessing, R. H. *J. Appl. Crystallogr.* **1997**, *30*, 421–426.
- (20) Sheldrick, G. M. *SHELXL97*, v6.10, University of Göttingen, Germany, 1996.
- (21) Koritszansky, T.; Howard, S. T.; Richter, T.; Macchi, P.; Volkov, A.; Gatti, C.; Mallinson, P. R.; Farrugia, L. J.; Su, Z.; Hansen, N. K. *Program XD*, 2003.
- (22) Allen, F. H.; Kennard, O.; Watson, D. G.; Brammer, L.; Orpen, A. G.; Taylor, R., *J. Chem. Soc., Perkin Trans. 2* **1987**, S1–S19.
- (23) Hirschfeld, F. L. *Acta Crystallogr.* **1976**, *A32*, 239–244.
- (24) Frisch, M. J.; et al. *Gaussian 03*, Revision B.05; Gaussian, Inc.: Pittsburgh PA, 2003.
- (25) (a) Becke, A. D. *J. Chem. Phys.* **1993**, *98*, 5648–5652. (b) Lee, C.; Yang, W.; Parr, R. G. *Phys. Rev. B* **1988**, *37*, 785–789.
- (26) (a) Peng, C.; Ayala, Y. P.; Schlegel, H. B.; Frisch, M. J. *J. Comput. Chem.* **1996**, *17*, 49–56. (b) Peng, C.; Schlegel, H. B. *Isr. J. Chem.* **1994**, *33*, 449–454.
- (27) (a) London, F. *J. Phys. Radium* **1937**, *8*, 397–409. (b) McWeeny, R. *Phys. Rev.* **1962**, *126*, 1028–1034. (c) Ditchfield R. *Mol. Phys.* **1974**, *27*, 789–807. (d) Wolinsky, K.; Sadlej, A. J. *Mol. Phys.* **1980**, *41*, 1419–1430. (e) Wolinsky, K.; Hinton, J. F.; Pulay, P. *J. Am. Chem. Soc.* **1990**, *112*, 8251–8260.
- (28) Biegler-König, F. W.; Schönbohm, J. *J. Comput. Chem.* **2002**, *23*, 1489–1494.
- (29) (a) Biegler-König, F. W.; Bader, R. F. W.; Tang, T. *J. Comput. Chem.* **1982**, *3*, 317–328. (b) A modified version of the PROAIMV-code was used including the Source Function (C. Gatti, unpublished).
- (30) Madsen, G. K. H.; Iversen, B. B.; Larsen, F. K.; Kapon, M.; Reiser, G. M.; Herbstein, F. H. *J. Am. Chem. Soc.* **1998**, *120*, 10040–10045.
- (31) (a) Wilson, C.; Iversen, B. B.; Overgaard, J.; Larsen, F. K.; Wu, G.; Pali, S. P.; Timco, G. A.; Gerbelau, N. V. *J. Am. Chem. Soc.* **2000**, *122*, 11370–11379. (b) Ammeter, J.; Bürgi, H. B.; Gamp, E.; Meyer-Sandrin, V.; Jensen, W. P. *Inorg. Chem.* **1979**, *18*, 733–750. (c) Stebler, M.; Bürgi, H. B. *J. Am. Chem. Soc.* **1987**, *109*, 1395–1401.
- (32) (a) Bolvig, S.; Hansen, P. E.; Wemmer, D.; Williams, P. J. *Mol. Struct.* **1999**, *509*, 171–181. (b) Hansen, P. E.; Bolvig, S. *Magn. Reson. Chem.* **1997**, *35*, 520–528.
- (33) In **2**, the right β -ketoenolic fragment does not have alternating single and double bonds, thus no λ -value is calculated.
- (34) The ^1H NMR chemical shifts were measured by ^1H MAS NMR at 9.4 T.
- (35) (a) Pacios, L. F.; Gómez, P. C. *J. Phys. Chem. A* **2004**, *108*, 11783–11792. (b) Alkorta, I.; Elguero, J.; Mó, O.; Yáñez, M.; Del Bene, J. E. *Mol. Phys.* **2004**, *102*, 2563–2574.
- (36) (a) Mildvan, A. S.; Massiah, M. A.; Harris, T. K.; Marks, G. T.; Harrison, D. H. T.; Viragh, C.; Reddy, P. M.; Kovach, I. M. *J. Mol. Struct.* **2002**, *615*, 163–175. (b) Bertolasi, V.; Gilli, P.; Ferretti, V.; Gilli, G. *J. Chem. Soc., Perkin Trans 2* **1997**, 945–952.
- (37) Popelier, P. *Atoms in Molecules, An Introduction*; Prentice Hall/Pearson Education Ltd.: Essex, U.K., 2000.
- (38) Partasarathi, R.; Subramanian, V.; Sathyamurthy, N. *J. Phys. Chem. A* **2006**, *110*, 3349–3351.
- (39) Espinosa, E.; Lecomte, C.; E. Molins, E. *Chem. Phys. Lett.* **1999**, *300*, 745–748.
- (40) Abramov, Y. A. *Acta Crystallogr.* **1997**, *A53*, 264–272.